

Article

Numerical Study of Thermochemistry and Trace Element Behavior during the Co-Combustion of Coal and Sludge in Boiler

Di Liang , Yimin Li and Zhongning Zhou *

School of Low-carbon Energy and Power Engineering, China University of Mining and Technology, Xuzhou 221116, China; turbo@cumt.edu.cn (D.L.); liyimin@cumt.edu.cn (Y.L.)

* Correspondence: zznwt@163.com

Abstract: Sludge is one of the main pollutants from sewage treatment and contains a high content of water and organic matter. The co-combustion of sludge and coal can bring about the energy conversion of sludge. However, the high moisture content in sludge and the inorganic pollutants generated by co-combustion have adverse effects on combustion and the environment. In this work, through experimentation, it was demonstrated that co-combustion does not release obvious toxic elements or create an environmental hazard. On the basis of the TG/DTG curves, the ignition points of sludge and coal and the temperature of each group were obtained, which provided boundary conditions for a numerical simulation. Co-combustion with various mixing ratios and moisture contents was studied via the numerical simulation of a 330 MW boiler. The numerical results show that a high mixing ratio reduced the boiler temperature and created more moisture and fuel NO_x. When the mixing ratio reached 40%, the boiler temperature became less than the combustion temperature. Sludge drying improved the internal temperature of the boiler, but it created thermal NO_x. When the moisture content decreased to 40%, the temperature in the boiler rose, which improved combustion.

Keywords: sludge; co-combustion; toxic element; numerical simulation; moisture content



Citation: Liang, D.; Li, Y.; Zhou, Z. Numerical Study of Thermochemistry and Trace Element Behavior during the Co-Combustion of Coal and Sludge in Boiler. *Energies* **2022**, *15*, 888. <https://doi.org/10.3390/en15030888>

Academic Editor: Adam Smoliński

Received: 28 December 2021

Accepted: 24 January 2022

Published: 26 January 2022

Publisher's Note: MDPI stays neutral with regard to jurisdictional claims in published maps and institutional affiliations.



Copyright: © 2022 by the authors. Licensee MDPI, Basel, Switzerland. This article is an open access article distributed under the terms and conditions of the Creative Commons Attribution (CC BY) license (<https://creativecommons.org/licenses/by/4.0/>).

1. Introduction

Sludge treatment has become an important topic in current environmental protection research and is of great significance for environmental protection and ecological security. Currently, the most common methods to treat sludge are through landfills, agriculture, or incineration [1], among others. Incineration is one of the most thorough treatment methods [2] because it completely carbonizes and burns the organic matter, thereby destroying the pathogenic microorganisms in the sludge. Incineration also has the advantages of rapidity, no need for long-term storage, short transport distance, and significant volume reduction [3–7]. At present, two main treatment methods exist for sludge incineration [8]: Combustion and co-combustion.

Nadziakiewicz [9] studied the co-combustion of sludge and coal by thermogravimetric (TG) analysis and concluded that the substances contained in sludge strongly affect mixing and combustion. In actual co-combustion conditions, thermal power plants must strictly control the mixing ratio of sludge and the substances it contains. Folgueras et al. [10] pyrolyzed coal and sludge at a heating rate of 20 K/min after mixing it and found that the temperature at which the volatile powder precipitates from the mixture of pulverized coal and sludge lags behind that of single sludge, and the ignition point is delayed. Calvo et al. [11] studied the characteristic pyrolysis curve of sludge under different atmospheres and found no significant variation in sludge pyrolysis under these conditions.

In a practical example, Li et al. [12] explored the combustion of sludge as an alternative fuel for the cement industry. Sludge mainly combusts in the low-temperature stage and

its activation energy is less than that of coal. Tan et al. [13] studied the co-combustion characteristics of a 100 MW power plant through field experiments and reports that the best choice is to co-burn 10% sludge with a moisture content between 40% and 56%. Zhou et al. [14] studied the combustion characteristics of oily sludge in a laboratory-scale circulating fluidized bed. The characteristics provide information about the release and combustion position of volatile matter.

In addition, the inorganic pollutants produced by the co-combustion of sludge and coal also deserve attention. Li et al. [15] studied the reaction mechanism of H₂S formed by coal burning in air in stages through experiments, thereby establishing a sulfur release model and describing the relationship between sulfur release and coal type. Shen et al. [16] explored the process of conversion from coal ash to slag through experiments and a numerical simulation, and demonstrated the general relationship between the design temperature, ash liquid temperature, operating temperature, and slag polymerization degree. Ma et al. [17] used a two-stage fluidized bed reactor to determine the characteristics of nitrogen conversion and distribution in the two basic stages of coal conversion (pyrolysis and subsequent char gasification). Nowicki et al. [18,19] systematically studied the gasification of char derived from sludge and established kinetic parameters for sewage sludge char gasification. Chen et al. [20] studied the thermochemical and kinetic behavior of coal, municipal sludge (MS), and their mixed combustion in different proportions by thermogravimetric analysis and demonstrated that the co-combustion of coal and sludge can effectively reduce the volatilization rate of toxic elements. Li et al. [21] studied the combustion behavior of municipal and residual petrochemical sludge and their co-combustion characteristics using a differential thermal gravimetric (DTG) analysis and determined the optimal heating rate of a mixed sample combustion. Thus, mixing sludge and coal in a boiler for combustion is an effective sludge treatment. However, the high moisture content of sludge and the excessive co-combustion fraction strongly affect boiler operation, the thermal efficiency of combustion, and the combustion pollutants, even to the point of causing abnormal power generation. In addition, secondary pollutants generated through co-combustion pose a grave threat to public health and the environment. Therefore, it is vital to better understand the co-combustion characteristics of coal–sludge mixtures and the resulting pollutants.

2. Materials and Methods

2.1. Sample Preparation and Experimental Methods

The coal was supplied by a fuel company in Xuzhou and sewage sludge was supplied by a sewage treatment plant in Xuzhou. The equipment used in this work was all of Chinese origin. The drying oven was produced by Shanghai Jinghong Experimental Equipment Co. The mixer was made by Changzhou Putian Instrument Manufacturing Co. The vacuum drying oven was produced by Yancheng Kejie Experimental Instrument Factory. The thermogravimetric analyzer (TGA) was manufactured by Shanghai Tianmei Balance Instrument Co. The sludge sample was first dried in a constant-temperature drying oven at 105 °C for 24 h and then milled through a 120-mesh sieve. At different proportions, the mixed sample of coal powder and sludge—with a total mass of 200 g—was weighed and the sample was mechanically stirred in a beaker with water as the medium. After removing the water and milling through a 120-mesh sieve, the sample was stored in a vacuum drying oven. A thermogravimetric-differential thermogravimetric (TG-DTG) analyzer was used to analyze the coal and sludge. N₂ (99.99%) was used as the pyrolysis gas and dry air as the combustion gas at gas flow rates of 60 ml/min. The 12 ± 0.5 mg sample was heated to 1000 °C at various heating rates (10, 20, and 30 °C/min).

2.2. Experimental Results of Pyrolysis and Combustion

Figure 1a,b show the TG-DTG curve of coal and sludge with an 80% moisture content in the air, heated at a rate of 30 °C/min. Comparing the DTG curves of coal and sludge combustion revealed weight-loss peaks for coal near 330 and 550 °C. The temperature of 330 °C corresponds to the precipitation of Vdaf, whereas 550 °C corresponds to the combustion of carbon. The three weight-loss peaks of sludge appear at around 110, 385, and 605 °C. The temperature of 110 °C corresponds to the evaporation of water in sludge, 385 °C corresponds to the volatilization of organic matter in sludge, and 605 °C corresponds to the combustion of organic matter and carbon. When 10% sludge was added to the coal, the DTG curve essentially remained the same. When the co-combustion rate was increased, the DTG curve shifted down and the temperature of the first peak decreased. When the co-combustion rate reached 30%, three inflection points appeared in the DTG. Upon increasing the sludge mixing ratio, the properties of the blended samples approached those of sludge. Table 1 shows data for the co-combustion of sludge and coal under different mixing ratios, where T_s is the Vdaf temperature, T_i is the ignition temperature, $(dw/dt)_{max}$ is the maximum weight-loss rate, and T_h is the burnout temperature. According to Table 1, the ignition temperature of sludge is approximately 250 °C and that of coal is approximately 420 °C. The Vdaf temperature of sludge is 125 °C, which is significantly less than that of coal (260 °C). On the basis of the initial Vdaf temperature calculated for this experiment, the initial Vdaf temperatures of sludge and coal in the numerical simulation are defined as 400 and 535 K, respectively, and the ignition points of sludge and pulverized coal are defined as 525 and 695 K, respectively. The DTG and TG curves of the sludge pyrolysis process under an N₂ atmosphere are shown in Figure 1c,d. Compared with a dry-air atmosphere, the peak weight-loss temperature was higher in the N₂ atmosphere due to the presence of O₂ in the air atmosphere, which accelerated the pyrolysis reaction of the sludge and made the weight-loss temperature of the sludge peak sooner. The pyrolysis kinetics of solid fuels, such as sludge and coal, have been extensively studied and therefore will not be discussed in this work. Specific studies on the reaction kinetics mechanism can be found elsewhere [22,23].

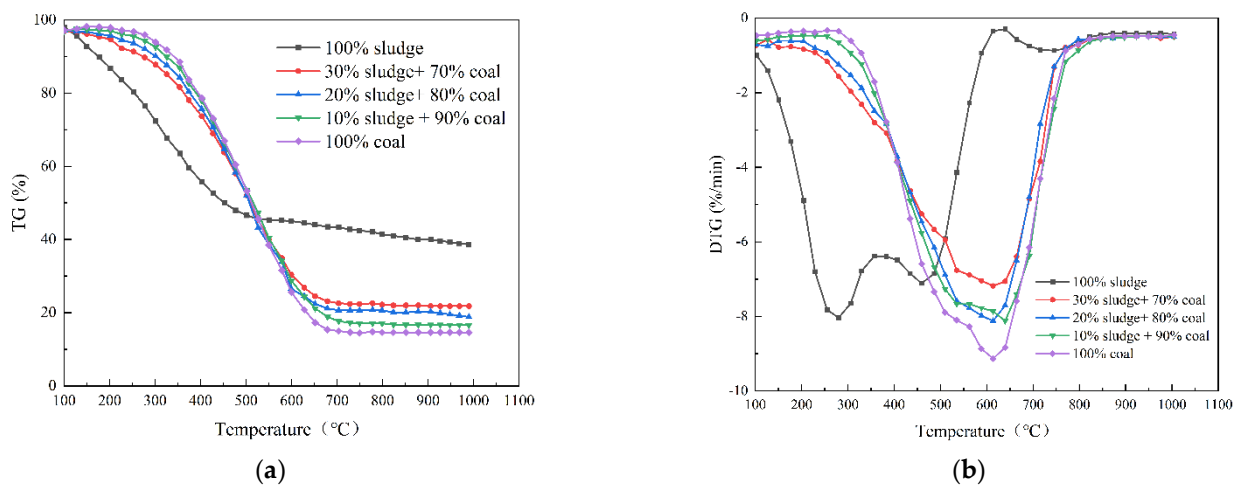


Figure 1. Cont.

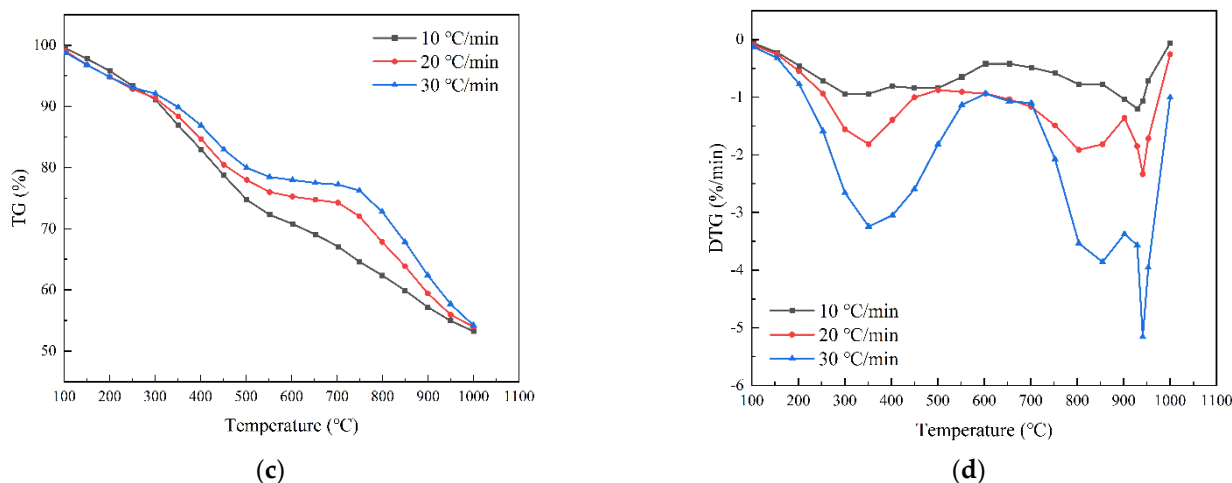


Figure 1. Co-combustion at different mixing ratios: (a) TG curve (dry gas atmosphere); (b) DTG curve (dry gas atmosphere); (c) TG curve (N₂ atmosphere); (d) DTG curve (N₂ atmosphere).

Table 1. Thermal analysis data of combustion at different mixing ratios.

Mixing Ratio (%)		T_s (°C)	T_i (°C)	$(dw/dt)_{max}$ (%/min)	T_h (°C)
Coal	Sludge				
100	0	260	420	−9.1	779.46
90	10	218	413	−8.31	782.53
80	20	200	414	−8.21	786.45
70	30	185	410	−7.25	783.52
0	100	135	248.58	−8.24	791.88

2.3. Migration Characteristics of Elements

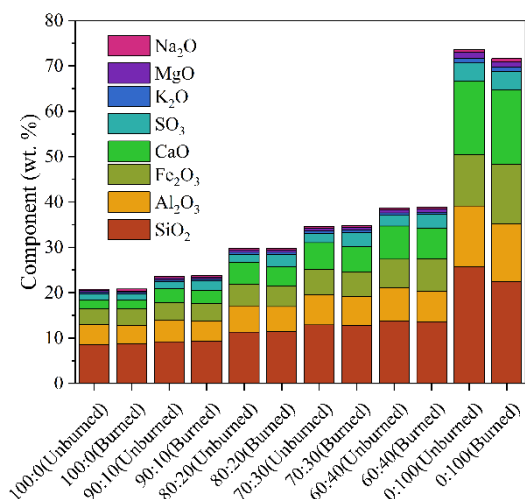
Considering the complex composition of and the potential environmental pollution caused by sludge, it is necessary to evaluate the environmental influence of sludge and coal in co-combustion, which can be determined by the variation of components in the sample before and after combustion. Coal and sludge were mixed in a certain ratio and divided into unburned and burned experimental groups. The method of coning and quartering was used to sample the sludge and coal, which had been tested five times for composition. The variance and standard deviation of all the data were calculated to measure the uncertainty of the corresponding data. The average of five measurements and uncertainty were shown as “A ± B” in Table 2, where “A” is the average of five measurements and “B” is the uncertainty. In addition, analyses of variance (ANOVA) were applied to verify the differences of the data based on the results of the variance calculation. The corresponding ratios were converted for the components of the sample after combustion due to the fact that volatile fractions, such as carbonaceous organics, are lost during the combustion process. A similar treatment was used for the analysis of trace elements in the samples, and the results are shown in Table 3. The comparison of the composition analysis and trace element analysis is shown in Figure 2.

Table 2. Component analysis of each proportion in samples before and after combustion.

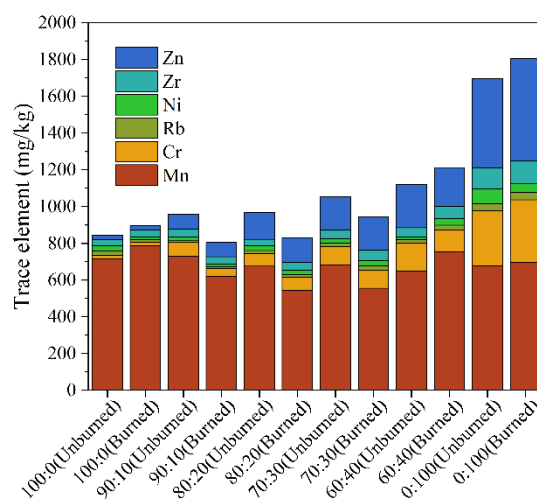
Mixing Ratio (Coal: Sludge, wt. %)	Analysis of Variance (F-Value)	Component (wt. %)							
		SiO ₂	Al ₂ O ₃	Fe ₂ O ₃	CaO	SO ₃	K ₂ O	MgO	Na ₂ O
100:0 (Unburned)	0.000482	8.52 ± 0.08	4.41 ± 0.09	3.50 ± 0.14	1.87 ± 0.08	1.35 ± 0.06	0.41 ± 0.03	0.38 ± 0.05	0.34 ± 0.03
100:0 (Burned)	0.000359	8.71 ± 0.12	4.12 ± 0.13	3.64 ± 0.17	1.88 ± 0.11	1.33 ± 0.08	0.35 ± 0.02	0.32 ± 0.02	0.44 ± 0.03
90:10 (Unburned)	0.001773	9.19 ± 0.13	4.66 ± 0.09	3.95 ± 0.14	3.11 ± 0.05	1.51 ± 0.10	0.42 ± 0.03	0.43 ± 0.05	0.33 ± 0.04
90:10 (Burned)	0.001936	9.29 ± 0.14	4.52 ± 0.16	3.82 ± 0.07	2.83 ± 0.08	2.11 ± 0.09	0.41 ± 0.03	0.40 ± 0.03	0.39 ± 0.04
80:20 (Unburned)	0.002379	11.32 ± 0.11	5.79 ± 0.14	4.82 ± 0.09	4.73 ± 0.15	1.73 ± 0.08	0.51 ± 0.05	0.55 ± 0.03	0.36 ± 0.03
80:20 (Burned)	0.000771	11.38 ± 0.17	5.55 ± 0.15	4.56 ± 0.14	4.15 ± 0.11	2.77 ± 0.12	0.49 ± 0.04	0.50 ± 0.03	0.42 ± 0.03
70:30 (Unburned)	0.001534	12.88 ± 0.18	6.67 ± 0.14	5.54 ± 0.09	5.93 ± 0.13	1.96 ± 0.07	0.59 ± 0.05	0.63 ± 0.02	0.39 ± 0.03
70:30 (Burned)	0.000416	12.73 ± 0.13	6.42 ± 0.15	5.35 ± 0.10	5.56 ± 0.13	3.16 ± 0.10	0.56 ± 0.06	0.58 ± 0.05	0.47 ± 0.01
60:40 (Unburned)	0.000738	13.79 ± 0.14	7.25 ± 0.11	6.31 ± 0.13	7.34 ± 0.13	2.32 ± 0.14	0.57 ± 0.01	0.69 ± 0.03	0.42 ± 0.02
60:40 (Burned)	0.000953	13.50 ± 0.20	6.75 ± 0.13	7.15 ± 0.08	6.75 ± 0.07	3.06 ± 0.17	0.56 ± 0.04	0.63 ± 0.04	0.45 ± 0.04
0:100 (Unburned)	0.000190	25.71 ± 0.08	13.41 ± 0.11	11.31 ± 0.18	16.18 ± 0.06	4.01 ± 0.17	1.05 ± 0.02	1.33 ± 0.02	0.61 ± 0.03
0:100 (Burned)	0.000338	22.44 ± 0.16	12.77 ± 0.12	13.13 ± 0.13	16.36 ± 0.13	4.06 ± 0.05	0.93 ± 0.02	1.18 ± 0.07	0.71 ± 0.05

Table 3. Trace element analysis of each proportion in samples before and after combustion.

Mixing Ratio (Coal: Sludge, wt. %)	Analysis of Variance (F-Value)	Trace Element (mg/kg)					
		Mn	Cr	Rb	Ni	Zr	Zn
100:0 (Unburned)	0.000459	716 ± 11	17 ± 5	26 ± 4	28 ± 4	32 ± 11	26 ± 3
100:0 (Burned)	0.000208	788 ± 4	19 ± 4	11 ± 2	14 ± 2	41 ± 1	22 ± 5
90:10 (Unburned)	0.000886	731 ± 11	73 ± 7	9 ± 1	21 ± 2	41 ± 4	83 ± 3
90:10 (Burned)	0.000437	621 ± 9	41 ± 1	10 ± 2	16 ± 3	39 ± 4	77 ± 1
80:20 (Unburned)	0.000785	675 ± 13	69 ± 2	16 ± 3	26 ± 3	36 ± 2	146 ± 1
80:20 (Burned)	0.001153	544 ± 8	72 ± 3	13 ± 4	23 ± 1	45 ± 2	133 ± 3
70:30 (Unburned)	0.000016	681 ± 4	100 ± 1	19 ± 2	25 ± 3	46 ± 2	184 ± 2
70:30 (Burned)	0.001143	555 ± 14	100 ± 2	22 ± 2	28 ± 1	57 ± 2	181 ± 2
60:40 (Unburned)	0.000881	649 ± 12	151 ± 1	18 ± 2	16 ± 2	50 ± 1	236 ± 3
60:40 (Burned)	0.000678	754 ± 11	119 ± 2	25 ± 1	34 ± 3	69 ± 1	211 ± 1
0:100 (Unburned)	0.000024	678 ± 10	298 ± 4	39 ± 4	82 ± 1	112 ± 2	487 ± 1
0:100 (Burned)	0.000123	698 ± 5	338 ± 3	42 ± 3	44 ± 3	126 ± 1	558 ± 3



(a)



(b)

Figure 2. The comparison of the composition analysis and trace element analysis: (a) composition; (b) trace element (mixing ratios is coal to sludge).

The ANOVA results (F-value) of all samples were observably smaller than the F-critical value. This means that there is no significant difference between tests corresponding to each group of samples. Furthermore, the uncertainty data indicate that the overall remained within a reasonable range. Combined with the ANOVA results, it can be concluded that the data can reflect the trend in the real situation.

Table 2 and Figure 2a suggest that the primary inorganic chemical components in coal are SiO₂, Al₂O₃, and Fe₂O₃, whereas those in sludge are SiO₂, Al₂O₃, Fe₂O₃, and

alkali oxides including CaO, K₂O, MgO, and Na₂O. It has previously been observed that the high concentration of alkali oxides contained in sludge can induce agglomeration, which affects the co-combustion of coal [20,21]. According to Figure 2a, we found that the content of each component increased gradually with the proportion of sludge in both the unburned and burned samples, especially SiO₂ and CaO—which increased significantly. This phenomenon implies an increase of the ash or fly ash content in the boiler, which is detrimental to the efficient operation of the boiler. Therefore, it is necessary to find an optimal range of the sludge blending ratio in the simulation process in this work.

As a result of the low amounts of carbon contained in sludge, an increase in the proportion of sludge obviously reduces the organic carbon content, and thus the heat production, as compared to a sample of the same mass, while the content of each inorganic substance increases. This analysis is consistent with the simulation results in the following.

Similarly, the ANOVA results (F-value) of the trace elements were significantly smaller than the F-critical value, indicating that there was no significant difference between the five test results. Moreover, the uncertainty analysis results are satisfactory. In summary, the test results can be considered to be scientifically significant and credible.

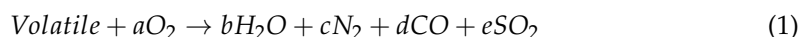
As is shown in Table 3 and Figure 2b, both coal and sludge contain similar levels of Mn and Rb, so the content of the above elements did not change significantly with an increasing mixing ratio. The sludge contained significantly larger amounts of Cr, Zr, Ni, and Zn, and the content of these elements observably increased with the increase in the mixing ratio.

Although the contents of these toxic elements are extremely low, special attention needs to be paid to the variation in toxic elements, which poses a potential threat to humans, plants, and animals [24]. Fortunately, Tables 2 and 3 and Figure 2 illustrate that both the oxides and trace elements contained in different proportions in the samples essentially remain constant before and after combustion. This indicates that each element is stably stored in the post-combustion products as oxides, which is consistent with the results reported by Moradian et al. [25]. These findings suggest that there is no significant release of toxic elements or environmental hazards from the co-combustion of sludge and coal, which should be further researched.

2.4. Numerical Calculation

In this paper, ANSYS FLUENT was used to simulate the flow, heat transfer, and combustion in a boiler. A non-premixed combustion model was used for the numerical simulation. The flow field of the boiler was simulated by Realizable $k - \epsilon$, and the eddy dissipation model (EDM) was introduced to simulate a volatile combustion. When establishing the EDM model, a two-step reaction was set. The first step was the formation of CO and other products. The second step was the combustion of CO. During the chemical reaction calculation with the EDM model, the volatile matter combustion process in coal and sludge was obtained according to the industrial analysis and elemental analysis of the pulverized coal and sludge, and the chemical reaction coefficient and standard enthalpy of volatile matter formation were determined. The chemical reaction process is as follows:

First step:



Second step:



When the volatile is regarded as $\text{Volatile} \cdot x\text{H}_2\text{O}$, the chemical reaction becomes:



In order to increase the accuracy of the numerical calculation, the boiler was divided into the bottom ash hopper area, the main burner area, the burnout area on the upper part of the furnace, and the platen superheater area, and a grid was drawn for each area. To eliminate pseudo-diffusion in the numerical calculation, the grids for the main combustion

area and the nozzle area were densified, as shown in Figure 3. After several cold-state calculations, the final number of the grid elements was 2.55×10^6 .

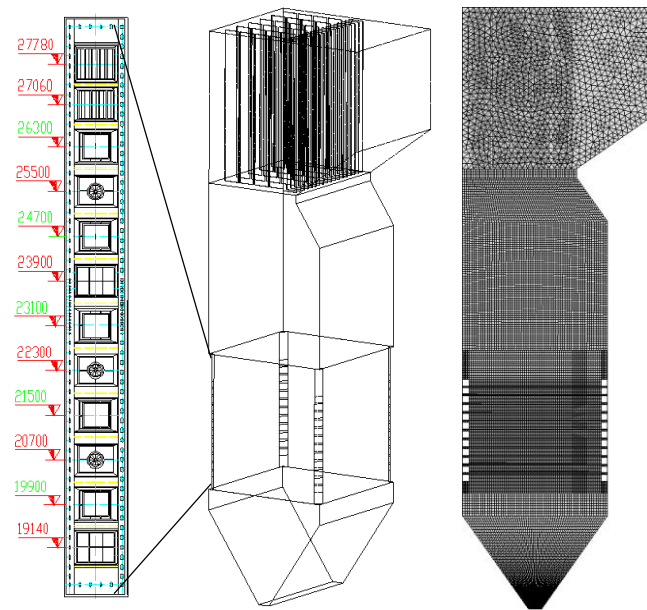


Figure 3. Boiler model and mesh.

2.5. Entrance Boundary Conditions

The velocity, temperature, and composition of the gas at the inlet boundary were directly given according to the design parameters of the boiler. The velocities of the primary air and secondary air were 25 and 45 m/s, respectively. The velocity direction was determined by the tangential angle of the burner. The hydraulic diameter H and turbulence intensity were calculated on the inlet boundary:

$$H = \frac{2A}{C}, \quad (4)$$

$$I \cong 0.16(Re_{HD})^{-1/8} \quad (5)$$

where A is the entrance area and C is the perimeter of the inlet surface. I is the turbulence intensity.

We used the Eddy dissipation model (EDM) to perform an element and industry analysis of the physical and chemical properties of the fuel. The settings are given in Table 4.

Table 4. Industry and element analysis in the EDM model.

Analysis Method	Abbreviation	Name	Coal	Sludge
Industry analysis	Mar	Moisture	14.00	80.10
	Aar	Ash	11.00	11.40
	Var	Volatile compound	27.40	7.63
	FCar	Fixed carbon	47.60	0.95
	HCV (MJ/kg)	High Calorific Value	23.90	8.21
Element analysis	C	Carbon	80.44	37.18
	H	Hydrogen	4.08	6.41
	O	Oxygen	13.25	44.29
	N	Nitrogen	0.93	6.53
	S	Sulfur	0.55	5.59

For the governing equation of the solid phase, the particle diameter followed the Rosin-Rammler distribution. The injection was set at the primary and secondary air inlet as the combustion inlet. The working conditions determined the fuel inlet temperature, specific heat, and density. The initial temperature of the sludge was denoted by T and that of the coal was denoted by T_s . The ignition temperature T_i was input as the boundary condition for the fuel. The velocity of the particles at the inlet was determined by the boiler combustion condition of 120 t/h. The temperature was determined by the primary and secondary air temperature. The boiler outlet boundary condition was set to that of the pressure outlet. Considering that, in actual operation, the boiler generally operated in negative pressure, and the outlet pressure was set to -80 Pa according to the design parameters of the boiler and the calculation of the boiler flue gas and air resistance. The wall of the furnace was a stationary, no-slip wall. The temperature, heat-transfer coefficient, and radiation coefficient of the boiler were all given. The boundary conditions of the burner wall were secondary-type boundary conditions: the temperature was 600 K, the heat-transfer coefficient was 450 W/m^2 , the radiation coefficient was 0.6, and the heat flux at the bottom ash hopper was zero. The temperature of the front platen superheater and the rear platen superheater were fixed at the actual working temperature (893.15 K), and the radiation coefficient was 0.4.

3. Results

As shown in Figure 4, with a mixing ratio of zero (in this work, the mixing ratio was the proportion of sludge to the total sample), the temperature of the outlet flue gas of the boiler was 1435 K (1162 °C), which was consistent with the actual temperature of the outlet flue gas of the boiler. The results show that the co-combustion of sludge significantly affected the flue-gas temperature at the boiler outlet, and the decreasing rate of the flue-gas temperature at the boiler outlet increased upon increasing the mixed combustion of sludge. When the mixing ratio increased from 0% to 20%, the flue-gas temperature at the boiler outlet only decreased by 98 °C. When the mixing ratio increased to 30%, the flue-gas temperature at the furnace outlet decreased by 240 °C. When the mixing ratio reached 40%, the flue-gas temperature at the boiler outlet was insufficient, indicating an incomplete combustion.

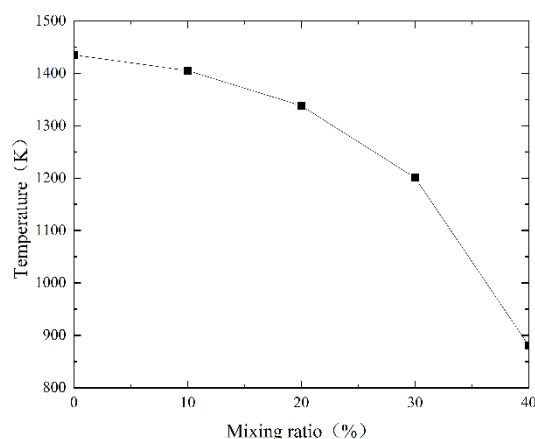


Figure 4. Flue-gas temperature at boiler outlet.

Figure 5 shows the temperature contours of the primary air in the lowest layer of the burners ($z = 20$ m) for several mixing ratios. When the mixing ratio was less than 40%, the combustion in the main combustion area of the burner was sufficient and the flame circle was consistent with the working condition. As well, the combustion position with respect to the boiler wall was appropriate and the temperature distribution was uniform. No local high-temperature regions existed near the wall and no high-temperature pulverized coal brushed the wall. Upon increasing the sludge mixing ratio, the temperature of the primary

air decreased, and the high-temperature area decreased, especially when the mixing ratio reached 40%. This trend was consistent with the phenomenon reported by Tan et al. [13]. When the mixing ratio increased from 0% to 40%, the maximum flame temperature in the boiler center decreased from 1792 to 882 K. When the mixing ratio reached 40%, the combustion in the boiler was not complete and the temperature in the boiler could not support normal combustion. Due to the high moisture and high ash content in the sludge, the fuel combustion was not sufficient and a lot of heat was lost through evaporation from the sludge in the burner area, which absorbed the heat generated by the fuel combustion. In addition, the high ash content of the sludge also decreased the calorific value of the fuel, so the final temperature in the burner area dropped sharply.

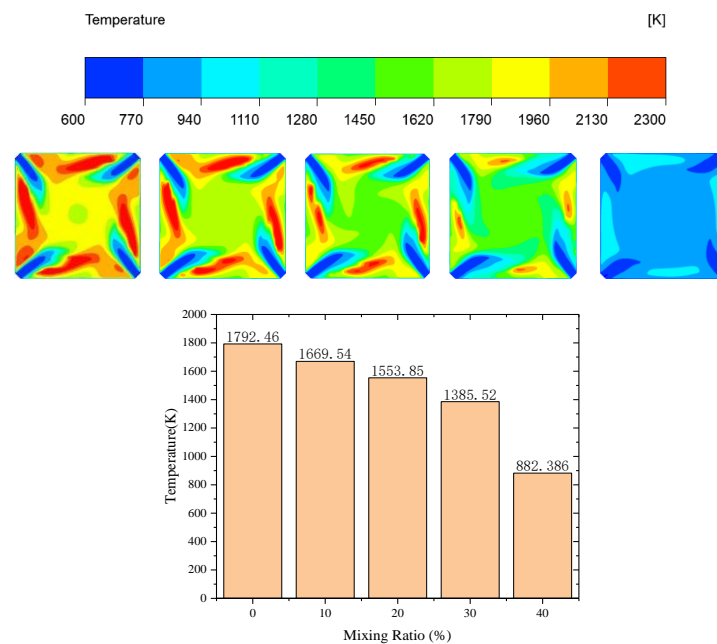


Figure 5. Temperature distribution of next wind section for various mixing ratios. From left to right, the mixing ratio is 0%, 10%, 20%, 30%, and 40%.

Figure 6a shows the H₂O distribution in the boiler for various mixing ratios. From left to right, the mixing ratio is 0%, 10%, 20%, and 30%. When the moisture content of the sludge reached 80%, with the increased co-combustion, more water entered the furnace and the moisture content in the furnace increased as co-combustion increased. Figure 6 shows that as co-combustion increased, the combustion of blended fuel worsened and the boiler temperature decreased; thus, the evaporation and heat absorption of water becomes an important factor that cannot be ignored. When the proportion of sludge in the mixed combustion exceeded 40%, combustion in the boiler was not sufficient and flameout became a possibility. As shown in Figure 6b when the amount of mixed combustion increased, the H₂O concentration in the boiler also increased. The H₂O in the boiler was mainly concentrated in the burner area. A large amount of C in the sludge affects the combustion of the fuel in the boiler, resulting in poor combustion, which adversely impacts the operation of the boiler.

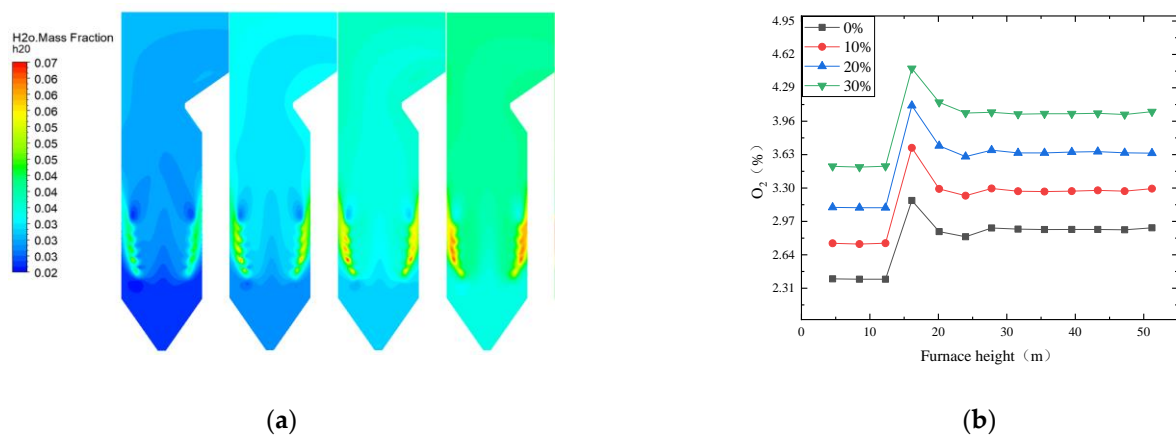


Figure 6. Moisture content in the boiler. (a) H₂O concentration in the center of the boiler for various mixing ratios. From left to right, the mixing ratio is 0%, 10%, 20%, and 30%. (b) H₂O concentration as a function of furnace height along the center of the boiler. The legend gives the mixing ratio.

Figure 7 shows the CO₂ distribution in the central section of the boiler for various mixing ratios. The mixing ratios from left to right are 0%, 10%, 20%, and 30%. When the mixing ratio was less than 30%, the average concentration of CO₂ in the boiler increased with height and CO₂ accumulated near the burner. Upon increasing the mixing ratio to 30%, the CO₂ concentration decreased near the burner.

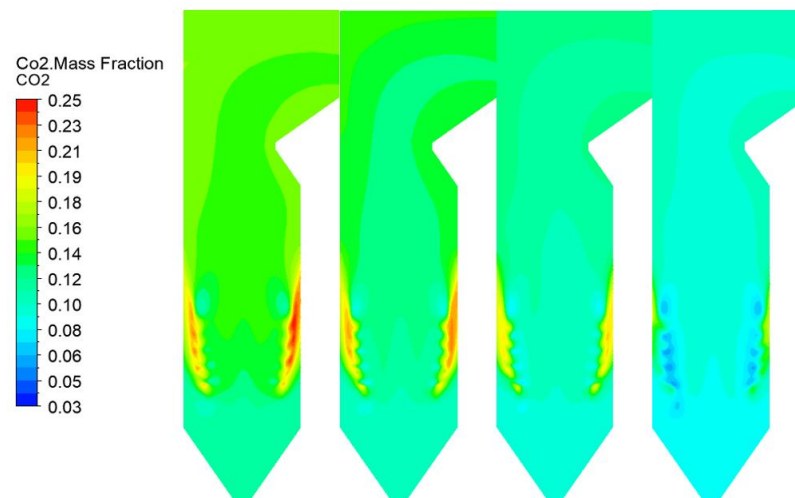


Figure 7. CO₂ distribution in the center of the boiler for various mixing ratios. From left to right, the mixing ratio is 0%, 10%, 20%, and 30%.

Figure 8 shows the distributions of CO₂, CO, and O₂ at different heights of the central section of the boiler and for various mixing ratios. In general, the average CO₂ concentration increased with boiler height. In the burner area, CO₂ increased with height, which is consistent with the trend shown in Figure 7. However, the CO₂ concentration in the burner area was not completely consistent under the different mixing ratios. When the mixing ratio was less than 20%, the CO₂ concentration followed an upward convex trend; however, when the mixing ratio exceeded 20%, the CO₂ concentration followed a downward convex trend, as shown in Figure 8a.

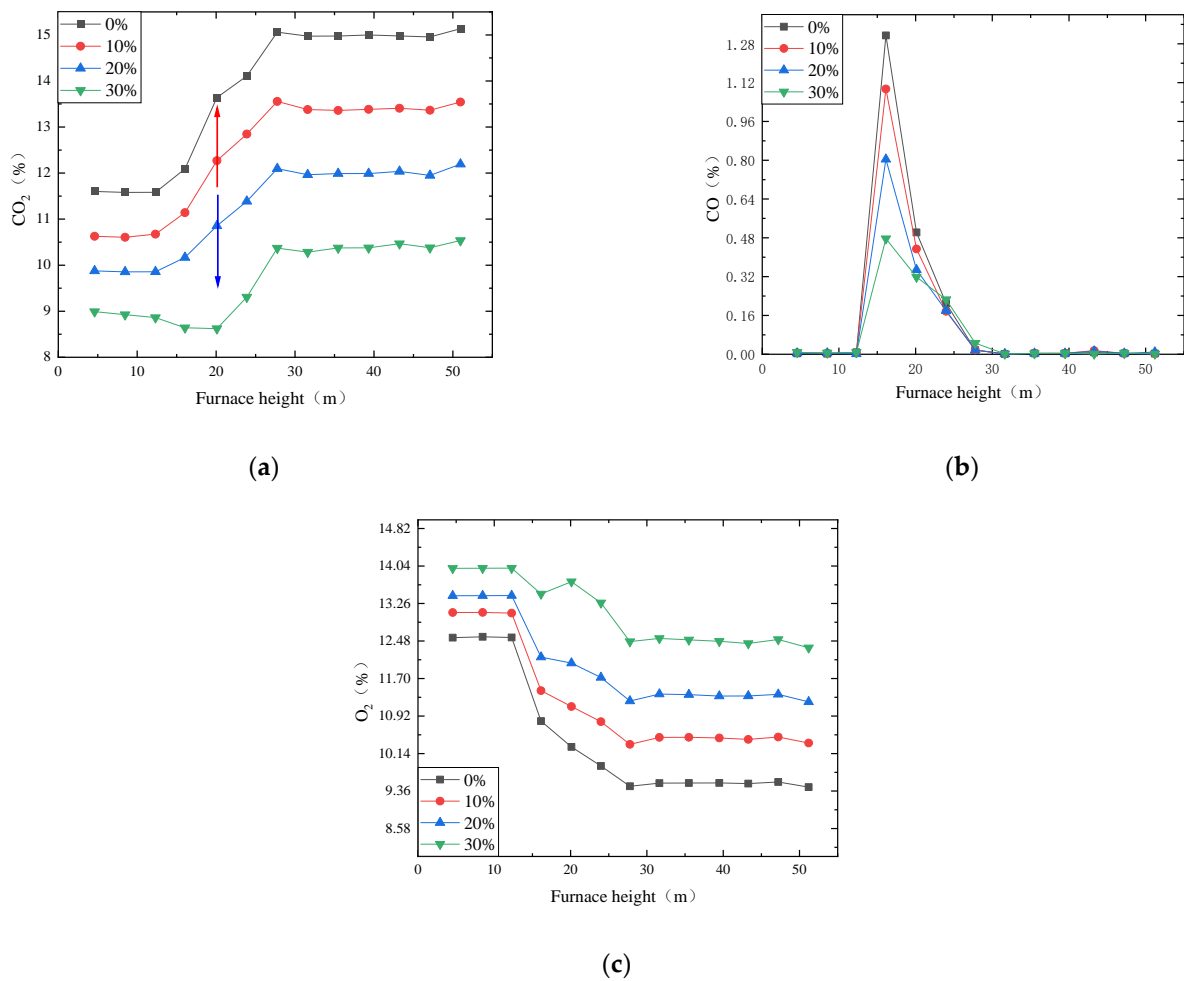


Figure 8. Gas distribution in the boiler with different mixing ratios: (a) CO₂; (b) CO; (c) O₂.

Figure 8b shows that CO was mainly distributed near the burner. When the mixing ratio was 30%, the CO content decreased to 0% at approximately 32 m. When the mixing ratio was less than 30%, the CO content decreased to 0% at approximately 27 m. Figure 8a,b suggest two reasons for this phenomenon: (1) given the increased mixing ratio, the content of volatiles and carbon in the fuel decreases, the concentration of CO₂ generated by combustion decreases, and the excess air dilutes the generated CO₂; (2) given the increased moisture content, the evaporation of a large amount of moisture removes the excess heat, and the volatiles and carbon do not completely separate at this temperature. Full combustion reduces the CO₂ concentration at the burner. Therefore, upon increasing the mixing ratio, the concentration of CO₂ and CO in the furnace decreased overall. With the increased mixing ratio, the O₂ distribution in the boiler followed a downward convex trend when the mixing ratio was less than 20% and an upward convex trend when the mixing ratio exceeded 20%. These results are similar to those of Manwatkar et al. for sludge combustion emission characteristics [26].

Figure 9 shows the NO_x distribution as a function of height in the boiler. Upon increasing the mixing ratio, the NO_x concentration at the bottom of the boiler increased because the N content of the sludge far exceeded that of the coal. The increased mixing ratio led to an increase in fuel NO_x. At the burner position in the boiler, the NO_x concentration increased at the same time, but the growth rate of NO_x concentration depended on the mixing ratio.

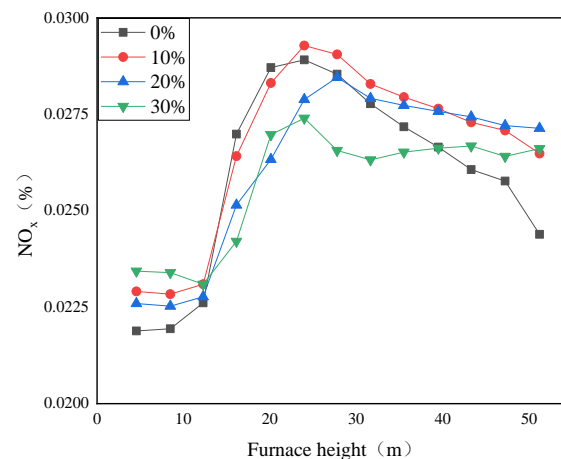


Figure 9. NOx concentration as a function of height along the center of the boiler. The legend gives the sludge mixing ratio.

Two types of NOx existed in the furnace: fuel NOx and thermal NOx. Near the burner, on the one hand, the mixed combustion of sludge increased fuel NOx; on the other hand, the thermal NOx decreased due to the evaporation and heat absorption of water in the sludge. Therefore, the total amount of NOx depended on the mixing ratio. When the mixing ratio was 10%, the furnace temperature remained high, and the total amount of thermal NOx and fuel NOx was maximal. When the mixing ratio exceeded 10%, the growth rate of thermal NOx was less than that of fuel NOx, so the overall trend was upward. When the mixing ratio reached 30%, the NOx did not decrease in the bottom layer of the burner. There are two main factors that explain this phenomenon: (1) incomplete combustion caused by the high mixing ratio and a reduction in fuel-type NOx; and (2) a low rate of thermal-type NOx generation caused by the low furnace temperature. When the mixing ratio was 20%, the NOx emission was the largest, increasing by approximately 11.3%. This finding is consistent with the report of Chen et al. [27].

Given that the moisture content of sludge can be as high as 80%, it can seriously affect the stable operation and pollutant emissions of the boiler; thus, reducing the moisture content of sludge improves the furnace temperature and fuel-burnout rate. Figure 10 shows that, with the decrease in moisture content in sludge, the flue-gas temperature at the furnace outlet increased and the rate of temperature increase gradually slowed, with the maximum temperature rate occurring at a 40% moisture content. Decreasing the moisture content from 80% to 20% caused the boiler outlet temperature to increase by approximately 108 K, which effectively improved the burnout rate of the fuel.

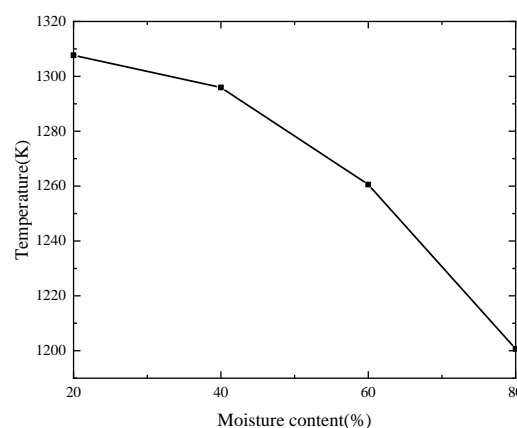


Figure 10. Flue-gas temperature at the boiler outlet as a function of moisture content.

Figure 11a shows the increased CO₂ concentration at the bottom of the furnace with an 80% moisture content, whereby the CO₂ concentration decreased near the burner. This is attributed to the lower furnace temperature at the bottom burner and the high moisture-content fuel absorbing a lot of heat at the bottom burner, which affected the normal combustion of the fuel. Therefore, given the decrease in CO₂ concentration at the bottom burner, the corresponding O₂ concentration increased, as shown in Figure 11c. Reducing the moisture content of the fuel to 60% decreased the influence of the moisture content at the bottom burner and the CO₂ concentration at the burner increased with height in the furnace. Upon decreasing the moisture content, the furnace temperature increased and the concentration of the intermediate product increased, as shown in Figure 11b. When the moisture content was 80%, the CO content decreased to 0% at approximately 32 m. When the moisture content was less than 60%, the CO content decreased to 0% at approximately 27 m.

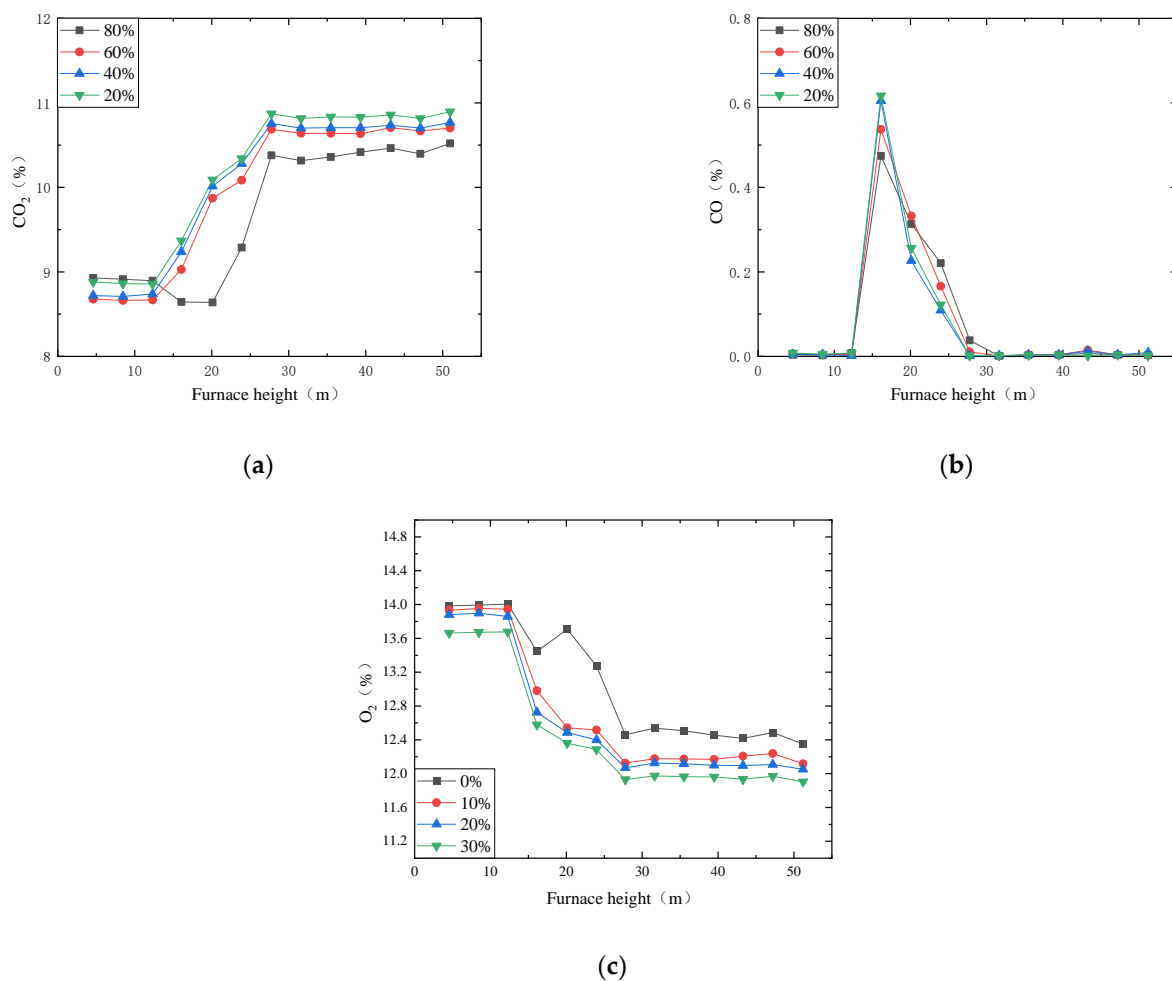


Figure 11. Gas distribution in the boiler as a function of furnace height and for various moisture contents: (a) CO₂; (b) CO; (c) O₂.

Figure 12 shows the average NO_x distribution at the cross-section through the furnace center. The total amount of fuel NO_x in the furnace remained unchanged due to the 30% mixing ratio. In general, as the furnace height increased, the NO_x production in the furnace increased. In the furnace burner area, the thermal NO_x production was larger due to the high temperature in this area. In the burnout wind area, the total amount of NO_x was maximal. The lower average temperature in the furnace under an 80% moisture content, and especially at the burner position, produced a slightly lower NO_x generation rate than under the four other working conditions. With the continuous rise in the furnace height,

the NO_x content gradually stabilized. Therefore, when the mixing ratio was fixed, the moisture content of the sludge decreased, and the temperature of the furnace burner area increased. Given the high temperature, thermal NO_x generation increased, which increased the NO_x content. When the moisture content decreased to 20%, the NO_x released increased by 32.9%. Tan et al. [28] suggested that high moisture in sludge promotes NO formation, leading to increased NO emissions after sludge co-combustion, which is consistent with the results of this work.

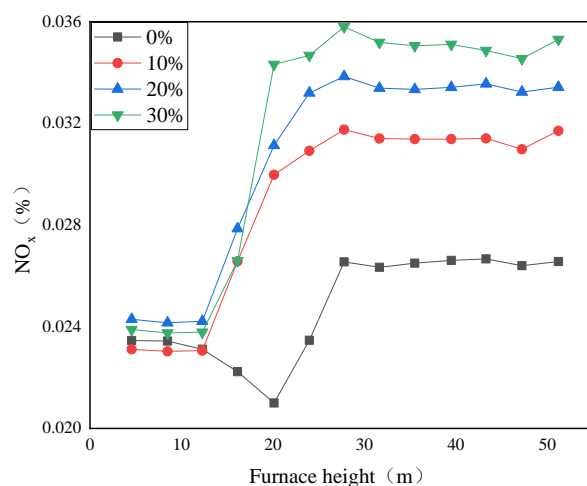


Figure 12. NO_x distribution as a function of furnace height along the center of the furnace.

4. Conclusions

Compared with samples of the same weight, the increase in sludge proportion significantly reduced the organic carbon content, thus reducing the heat production and increasing the content of each inorganic substance. However, all kinds of toxic elements are stored in the post-combustion products as oxides. Therefore, there is no release of harmful inorganic substances in the mixed combustion of sludge.

Sludge reduces the initial temperature T_s of fuel and its ignition temperature T_i . The burnout temperature T_h of the fuel increased. Due to the different compositions, two weight-loss peaks appeared for coal and three weight-loss peaks appeared for hydrous sludge. When the mixing ratio reached 30%, the third weight-loss peak appeared for coal, and sludge began to affect fuel combustion.

Given a constant moisture content of sludge, the increase in the sludge mixing ratio decreased the furnace temperature. The change in the boiler outlet temperature did not decrease linearly. When the mixing ratio increased from 0% to 20%, the flue-gas temperature at the boiler outlet only decreased by 98 °C. When the mixing ratio changed to 30%, the flue-gas temperature at the boiler outlet decreased by 240 °C. When the mixing ratio reached 40%, the furnace could not maintain normal combustion; thus, we recommend that the mixing ratio does not exceed 40%. This change caused the thermal NO_x content to decrease and the fuel NO_x content to increase. When the mixing ratio was 20%, the NO_x emission was greatest, increasing by approximately 11.3%.

Given a constant mixing ratio, the moisture content of the sludge decreased, and the furnace temperature increased. When the moisture content decreased from 80% to 20%, the boiler outlet temperature rose by approximately 108K, which effectively improved the burnout rate of the fuel. In addition, this change caused the content of thermal NO_x to increase and the content of fuel NO_x to remain constant. When the moisture content decreased to 20%, the NO_x released increased by 32.9%.

Author Contributions: Conceptualization, Z.Z.; methodology, D.L. and Z.Z.; software, D.L.; formal analysis, D.L. and Z.Z.; investigation, D.L.; resources, D.L.; data curation, D.L.; writing—original draft preparation, D.L.; writing—review and editing, Z.Z.; visualization, D.L.; supervision, Y.L.; project administration, Y.L.; funding acquisition, Y.L. All authors have read and agreed to the published version of the manuscript.

Funding: This work was funded by the National Natural Science Foundation of China (Grant No. 51776217).

Institutional Review Board Statement: Not applicable.

Informed Consent Statement: Not applicable.

Data Availability Statement: Not applicable.

Conflicts of Interest: The authors declare no conflict of interest.

References

1. Folgueras, M.B.; Alonso, M.; Díaz, R.M. Influence of sewage sludge treatment on pyrolysis and combustion of dry sludge. *Energy* **2013**, *55*, 426–435. [[CrossRef](#)]
2. Werther, J.; Ogada, T. Sewage sludge combustion. *Prog. Energy Combust. Sci.* **1999**, *25*, 55–116. [[CrossRef](#)]
3. Kalisz, S.; Pronobis, M.; Baxter, D. Co-firing of biomass waste-derived syngas in coal power boiler. *Energy* **2008**, *33*, 1770–1778. [[CrossRef](#)]
4. Rulkens, W. Sewage sludge as a biomass resource for the production of energy: Overview and assessment of the various options. *Energy Fuels* **2007**, *22*, 9–15. [[CrossRef](#)]
5. Nzihou, A.; Flamant, G.; Stanmore, B. Synthetic fuels from biomass using concentrated solar energy—A review. *Energy* **2012**, *42*, 121–131. [[CrossRef](#)]
6. Pietrzak, R.; Bandosz, T.J. Interactions of NO₂ with sewage sludge based composite adsorbents. *J. Hazard. Mater.* **2008**, *154*, 946–953. [[CrossRef](#)] [[PubMed](#)]
7. Tingyu, Z.; Shouyu, Z.; Jiejie, H.; Yang, W. Effect of calcium oxide on pyrolysis of coal in a fluidized bed. *Fuel Process. Technol.* **2000**, *64*, 271–284. [[CrossRef](#)]
8. Tabasová, A.; Kropáč, J.; Kermes, V.; Nemet, A.; Stehlík, P. Waste-to-energy technologies: Impact on environment. *Energy* **2012**, *44*, 146–155. [[CrossRef](#)]
9. Nadziakiewicz, J.; Koziol, M. Co-combustion of sludge with coal. *Appl. Energy* **2003**, *75*, 239–248. [[CrossRef](#)]
10. Folgueras, M.B.; Díaz, R.M.; Xiberta, J.; Prieto, I. Thermogravimetric analysis of the co-combustion of coal and sewage sludge. *Fuel* **2003**, *82*, 2051–2055. [[CrossRef](#)]
11. Calvo, L.F.; Otero, M.; Jenkins, B.M.; García, A.I.; Morán, A. Heating process characteristics and kinetics of sewage sludge in different atmospheres. *Thermochim. Acta* **2004**, *409*, 127–135. [[CrossRef](#)]
12. Li, F.; Zhang, W. Combustion of sewage sludge as alternative fuel for cement industry. *J. Wuhan Univ. Technol. -Mater. Sci. Ed.* **2011**, *26*, 556–560. [[CrossRef](#)]
13. Tan, P.; Ma, L.; Xia, J.; Fang, Q.; Zhang, C.; Chen, G. Co-firing sludge in a pulverized coal-fired utility boiler: Combustion characteristics and economic impacts. *Energy* **2017**, *119*, 392–399. [[CrossRef](#)]
14. Zhou, L.; Jiang, X.; Liu, J. Characteristics of oily sludge combustion in circulating fluidized beds. *J. Hazard. Mater.* **2009**, *170*, 175–179. [[CrossRef](#)] [[PubMed](#)]
15. Li, Z.; Chen, H.; Zhang, Z. Experimental and modeling study of H₂S formation and evolution in air staged combustion of pulverized coal. *Proc. Combust. Inst.* **2021**, *38*, 5363–5371. [[CrossRef](#)]
16. Shen, Z.; Nikolic, H.; Caudill, L.S.; Liu, K. A deep insight on the coal ash-to-slag transformation behavior during the entrained flow gasification process. *Fuel* **2021**, *289*, 119953. [[CrossRef](#)]
17. Ma, J.; Tian, X.; Wang, C.; Zhao, H.; Liu, Z.; Zheng, C. Fate of fuel-nitrogen during in situ gasification chemical looping combustion of coal. *Fuel Process. Technol.* **2021**, *215*, 106710. [[CrossRef](#)]
18. Nowicki, L.; Markowski, M. Gasification of pyrolysis chars from sewage sludge. *Fuel* **2015**, *143*, 476–483. [[CrossRef](#)]
19. Nowicki, L.; Anteck, A.; Bedyk, T.; Stolarek, P.; Ledakowicz, S. The kinetics of gasification of char derived from sewage sludge. *J. Therm. Anal. Calorim.* **2010**, *104*, 693–700. [[CrossRef](#)]
20. Chen, Y.; Gui, H.; Xia, Z.; Chen, X.; Zheng, L. Thermochemical and toxic element behavior during co-combustion of coal and municipal sludge. *Molecules* **2021**, *26*, 4170. [[CrossRef](#)]
21. Li, J.; Hu, J.; Wang, T.; Gan, J.; Xie, J.; Shui, Y.; Liu, J.; Xue, Y. Thermogravimetric analysis of the co-combustion of residual petrochemical sludge and municipal sewage sludge. *Thermochim. Acta* **2019**, *673*, 60–67. [[CrossRef](#)]
22. Nowicki, L.; Siuta, D.; Markowski, M. Pyrolysis of rapeseed oil press cake and steam gasification of solid residues. *Energies* **2020**, *13*, 4472. [[CrossRef](#)]
23. Nowicki, L.; Siuta, D.; Markowski, M. Carbon dioxide gasification kinetics of char from rapeseed oil press cake. *Energies* **2020**, *13*, 2318. [[CrossRef](#)]

24. Teixeira, P.; Lopes, H.; Gulyurtlu, I.; Lapa, N.; Abelha, P. Evaluation of slagging and fouling tendency during biomass co-firing with coal in a fluidized bed. *Biomass Bioenergy* **2012**, *39*, 192–203. [[CrossRef](#)]
25. Moradian, F.; Pettersson, A.; Svärd, S.; Richards, T. Co-combustion of animal waste in a commercial waste-to-energy BFB boiler. *Energies* **2013**, *6*, 6170–6187. [[CrossRef](#)]
26. Manwatkar, P.; Dhote, L.; Pandey, R.A.; Middey, A.; Kumar, S. Combustion of distillery sludge mixed with coal in a drop tube furnace and emission characteristics. *Energy* **2021**, *221*, 119871. [[CrossRef](#)]
27. Chen, G.-B.; Chatelier, S.; Lin, H.-T.; Wu, F.-H.; Lin, T.-H. A study of sewage sludge co-combustion with Australian black coal and shiitake substrate. *Energies* **2018**, *11*, 3436. [[CrossRef](#)]
28. Tan, P.; Ma, L.; Fang, Q.; Zhang, C.; Chen, G. Application of different combustion models for simulating the co-combustion of sludge with coal in a 100 MW tangentially coal-fired utility boiler. *Energy Fuels* **2015**, *30*, 1685–1692. [[CrossRef](#)]